Available online at www.sciencedirect.com
SCIENCE DIRECT®
Journal of Molecular Catalysis A: Chemical 233 (2005) 133–139
JOURNAL OF MOLECULAR CATALYSIS A: CHEMICAL
www.elsevier.com/locate/molcata

Hydrogenation of edible oil over Pd-Me/Al_2O_3 catalysts (Me = Mo, V and Pb)

María B. Fernández, Cristian M. Piqueras, Gabriela M. Tonetto, Guillermo Crapiste, Daniel E. Damiani *

PLAPIQUI (UNS-CONICET), Camino La Carrindanga Km 7, CC 717, CP 8000, Bahía Blanca, Argentina

Received 21 December 2004; received in revised form 10 February 2005; accepted 14 February 2005

Abstract

This work presents the performance of supported Pd and Pd-Me (Me = Mo, V and Pb) catalysts in the hydrogenation of sunflower oil.

The catalysts were prepared using alumina as support, and were following two different methods of preparation: wet impregnating and sol–gel techniques. The samples were characterized by atomic absorption, N_2 adsorption isotherm, temperature-programmed reduction and hydrogen chemisorption.

For Pd monometallic catalysts prepared by wet impregnation (WI) of γ-Al_2O_3 and alumina sol–gel (SG), for the same iodine value (IV) and Pd surface, Pd-SG generates more *trans*-isomers than Pd-WI sample. This could be attributed to differences in the support morphology.

Regarding bimetallic catalysts, for a smaller amount of exposed Pd, the Pd-Mo/γ-Al_2O_3 and Pd-V/γ-Al_2O_3 catalysts show the same activity compared with the respective monometallic catalyst, and increase the selectivity to *trans*-isomers. The molybdenum and vanadium promoting effect could be a consequence of the formation of an adsorbed initial state, after which the hydrogenation would take place on the Pd surface.

On the other hand, Pd-Pb/γ-Al_2O_3 showed the lowest hydrogenation activity. This would be result of a certain dimensional limitations on the space lattice of Pd for hydrogenation of double bonds due to the formation of a Pd–Pb alloy.

The sol–gel Pd-Mo sample was the most effective catalyst regarding the *cis*-isomers selectivity and reveals the route for future research.
© 2005 Elsevier B.V. All rights reserved.

Keywords: Hydrogenation; Sunflower oil; *trans*-Isomers; Palladium; Molybdenum

1. Introduction

Hydrogenation of vegetable oils is an important practice in the modification of fats and oils. The hydrogenation process saturates part of the double bonds, while an important proportion of the remaining bonds is isomerized through the conversion *cis–trans* in the fatty acid chain. This process increases the melting temperature, increases the consistency for use as margarine and intensifies the resistance to oxidation [1].

From 1980, a good number of research works have been made in order to know the effect of *trans*-isomers of mono- and polyunsaturated fatty acids on the cellular metabolism. Kromhout et al. [2] presented a study in which 12,763 people were supervised during 25 years, demonstrating that the percentage of saturated fatty acids and *trans* fatty acids contained in the diet strongly correlated with the concentration of plasma cholesterol.

For this reason, the demand for smaller levels of *trans*-isomers content in hydrogenated edible oils has increased, and the search of alternatives is important to improve the hydrogenation process.

A field in which there have been major advances is that of hydrogenation catalysts [3]. The bulky size of the triglyceride molecules, together with the simultaneity of other reactions, as those of positional or geometric isomerization, can imply that the reaction could be sensitive to the catalytic structure. For this reason, supports have been designed with specific properties and a perfectly defined structure of pores [4], the

* Corresponding author. Tel.: +54 291 4861700; fax: +54 291 4861600.
E-mail address: ddamiani@plapiqui.edu.ar (D.E. Damiani).

1381-1169/$ – see front matter © 2005 Elsevier B.V. All rights reserved.
doi:10.1016/j.molcata.2005.02.012

Nomenclature

C	concentration (mol m^{-3})
D_{eff}	effective diffusion coefficient (m^2 s^{-1} × m^3 liquid m^{-3} catalyst)
r_{obs}	observed rate (mol s^{-1} kg^{-1} catalyst)
R	mean particle size (m)
TAG	triacylglyceride

Greek letters

Φ	Weisz–Prater criterion
ρ_p	catalyst apparent density (g/cm^3)

Subscripts and superscripts

i	component
p	particle

distribution of the particle size has been studied [33], and promoters and modifiers have also been used to improve the selectivity [5–7]. There are records for the use of Pd catalysts in the hydrogenation of edibles oils [8]. Because of higher activity than its Ni predecessors, the operation can be carried out under softer conditions.

The present work reports the hydrogenation of sunflower oil with Pd catalysts promoted with molybdenum, vanadium and lead. The aim was to compare the dependence of catalytic activity and selectivity with the support features and a second metal promotion, in order to corroborate the potential use of such catalysts in the industrial hydrogenation processes looking forward to obtaining a lower *trans*-isomer content in the hydrogenated edible oils.

2. Experimental

2.1. Catalysts preparation

The Pd-WI catalyst was prepared by impregnation of the γ-Al_2O_3 support (Condea, Puralox, 162.5 m^2 g^{-1}) with a solution of $Pd(C_5H_7O_2)_2$ (Alpha) in toluene. After the impregnation, the catalyst was dried in Ar at 150 °C for 2 h and then calcined in chromatographic air at 500 °C, for 2 h.

The PdMo-WI sample was prepared by co-impregnation of the metals on the γ-Al_2O_3 support using a solution of $Pd(C_5H_7O_2)_2$ and $MoO_2(C_5H_7O_2)_2$ (Alpha) in toluene. The sample was then dried and calcined as described above.

The synthesis of alumina xerogel and Mo-Al_2O_3 (hereinafter referred to as Al_2O_3-SG and Mo-SG, respectively) was carried out by sol–gel synthesis technique. Aluminum isopropoxide in 2-propanol solution was refluxed at 85 °C with constant stirring. For the preparation of the Mo-SG sample, the $MoO_2(C_5H_7O_2)_2$ in 2-propanol solution was added to the previous preparation at 85 °C with vigorous agitation, followed by the addition of water in a larger quantity than the stoichiometric amount. The reflux continued until the gel was formed. The resulting sol was dried at 110 °C for 18 h, and calcined at 550 °C for 5 h.

The Pd-SG sample was prepared in the same manner as the Pd-WI catalyst, using this Al_2O_3-SG as support.

In order to study the effect of Pb and V in the Pd/γ-Al_2O_3 hydrogenation activity, the reaction was tested in another two catalysts previously prepared and characterized in our laboratory. The Pd-Pb/γ-Al_2O_3 catalyst was prepared by reacting tetrabutyl-lead with a supported palladium sample derived from $Pd(C_5H_7O_2)_2$ as it is reported by Volpe et al. [39]. Pd-V/γ-Al_2O_3 sample was prepared by anchoring $Pd(C_5H_7O_2)_2$ to a V/γ-Al_2O_3 catalyst derived from NH_4VO_3 [9].

In every case, the supports were dried in N_2 at 150 °C during 2 h before the impregnation. The quantity of Pd precursor used was calculated to place approximately 1% of palladium by weight on the support. The Mo and V percentage was selected according a previous work [9,12]. The difference of Mo content between Pd-Mo catalysts was made on purpose.

2.2. Catalysts characterization

The metal (Pd, Mo, Pb and V) content was determined by atomic absorption spectroscopy (AAS).

In order to determine the specific surface area and the pore size and volume in bare supports, nitrogen adsorption isotherms were performed at 77 K using a volumetric system.

XRD pattern were collected using the powder method in a Rigaku diffractometer equipped with Cu Kα X-ray source and a Ni filter operated at 35 kV and 15 mA.

The H_2 chemisorption uptakes were measured in a conventional glass apparatus [10]. Before reduction, the catalysts were oxidized in air at 500 °C during 1 h. Then, the samples were purged in He and reduced at 250 °C in flowing H_2 for 1 h. Following reduction, the samples were evacuated for 20 h at reduction temperature and cooled to adsorption temperature (25 °C) under vacuum. Irreversible uptakes were determined from dual isotherms measured for hydrogen using the method of Benson et al. [11]. The fraction of exposed palladium was calculated assuming that one hydrogen atom is adsorbed per surface palladium atom.

TPR experiments were performed in a conventional apparatus, as previously described [12]. Before reduction, the catalyst (∼40 mg) was oxidized in flowing chromatographic air at 300 °C for 1 h and purged and cooled in Ar. Then, a mixture of 5% H_2 in Ar flow was then passed through the sample, and the temperature raised from −20 to 300 °C at a heating rate of 10 °C min^{-1}.

2.3. Catalytic activity measurements

Hydrogenation tests were carried out in a semibatch microreactor of 9 ml. The sunflower oil utilized in the catalytic activity measurements was a refined, bleached, and deodorized commercial sunflower oil. The reactor was connected

to a hydrogen (AGA grade chromatographic) source, maintained at constant pressure. A data acquisition cardboard connected to a PC was used to record the hydrogen flow originated as a result of the H_2 consumption during the reaction.

The catalyst sample was pre-reduced in situ at 400 °C. The sunflower oil was added to the reactor (containing the reduced catalyst at the reaction temperature) using a syringe. Then, the pressure was increased in order to start the reaction. Thus, the instantaneous H_2 consumption (a measure of the reaction rate) was obtained subtracting the hydrogen flow corresponding to the same operation but without reaction to the record of the hydrogen flow during the reaction.

The catalytic tests were performed at 100 °C and 60 psi during 1 h, using 8 ml of sunflower oil. The mass of catalyst employed in the reaction ranged between 100 and 200 mg and the stirring rate was 1400 rpm.

The analytical studies were performed with an AGILENT 4890D gas chromatograph (GC) equipped with a flame ionization detector (FID) following the procedures established by the AOCS Ce 1c-89 norm. A 60 m long SUPELCO 2380 capillary column, with a nominal diameter of 0.25 mm and a nominal film thickness of 0.20 μm was used for the separation of the different compounds present in the samples. The iodine number (IV) was calculated from the fatty acid composition following the AOCS Cd 1c-85 norm.

Because hydrogenation of edible oils is a three-phase process, several transport limitations may occur. The volumetric gas–liquid mass-transfer coefficient, $K_l a$, was separately measured at an excess of catalyst load [13]. Intraparticle diffusion limitations for Hydrogen were estimated from the Weisz–Prater number [14].

3. Results and discussion

3.1. Catalysts characterization

X-ray data of the alumina-SG sample calcined at 550 °C does not present any crystalline phase corresponding to alumina. This is an expected result according to the calcinations temperature used [15].

Other structural characteristics obtained from the nitrogen desorption at 77 K are presented in Table 1. The xerogel sample shows a specific surface area (327.5 $m^2\,g^{-1}$) similar to that reported in the literature [15–17]. It is also possible to note that Al_2O_3-SG sample exhibits a specific area that is twice as large as commercial γ-Al_2O_3.

Table 1
Supports properties

Sample	Specific surface area ($m^2\,g^{-1}$)	Pore volume (Å)	Pore diameter ($cm^3\,g^{-1}$)
γ-Al_2O_3	162.5	97.7	0.46
Al_2O_3-SG	327.5	63.6	0.54
Mo-SG	290.0	34.9	0.25

Mo-SG sample shows an important reduction in the pore volume and the pore diameter compared to Al_2O_3-SG sample. This would be consequence of the added Mo. On the other hand, no change in specific surface area or pore diameter is observed for γ-Al_2O_3 supported catalysts.

Table 2 lists the catalysts and their metal content determined by AAS. As mentioned in Section 2, the Pd-WI and Pd-SG samples were prepared from $Pd(C_5H_7O_2)_2$. It was reported [18] that the fixation of Pd acetylacetonate on alumina occurs by a ligand-exchange mechanism. A covalent bond is originated and HAcac ($C_5H_8O_2$) is generated, which remains adsorbed on the surface of alumina. When the catalyst precursor is calcined, the remaining $C_5H_7O_2$ ligand combusts and PdO particles are formed. This precursor originates metallic particles with high percentage of metal exposed. Table 2 shows that the amount of Pd fixed on Al_2O_3-SG is greater than the one fixed on γ-Al_2O_3, though both were precursor-impregnated under identical conditions. This could be attributed to a higher adsorption activity of the material. Since the specific surface area of the sol–gel derived sample is twofold higher than that of γ-Al_2O_3, Pd on alumina-SG is distributed over a larger surface.

The hydrogen chemisorption measurement results expressed as Pd exposed fraction are also summarized in Table 2. Assuming hemispherical particle and superficial density of 1.27×10^{19} Pd_s atoms/m^2, metal particle size in Pd-WI and Pd-SG catalysts is 2 and 2.8 nm, respectively ($d_p = 1.12/Pd_{exp}$) [19]. In relation to Pd monometallic catalysts, Pd-Mo bimetallic samples show a decrease in the H_2 chemisorption ability of Pd. During the preparation procedure, high oxidation temperature favors the formation of MoO_3, which after exposure to H_2 at high temperature reduces to a suboxide that tends to migrate onto the Pd surface, preventing its contact with H_2 [20,21]. FTIR spectroscopy measurements of NO and CO adsorbed on the catalysts corroborated this hypothesis [12].

The TPR results for the four Pd and Pd-Mo samples (pre-oxidized at 300 °C) are showed in Fig. 1. The profiles present a low temperature peak, between 25 and 50 °C, which is attributed to the reduction of palladium oxide. The high temperature peak (near 450 °C), in the bimetallic samples, corresponds to the partial reduction of MoO_3. The negative signal, near 60 °C, is originated in the decomposition of the

Table 2
Characterization of the catalysts: metallic contents, fraction of exposed Pd (from H_2 chemisorption), and H_2 consumed during TPR experiments

Sample	Pd (wt%)	Me (wt%)	Pd_s/Pd[a] (%)	H_2/Pd[b]
Pd-WI	0.82	–	56	1.2
Pd-SG	1.10	–	40	1.5
PdMo-WI	0.45	0.74	41	1.4
PdMo-SG	1.01	6.50	20	0.6
Pd–Pb	0.70	0.28	28	–
Pd-V	0.68	3.5	50	0.5

[a] Fraction of exposed palladium, H_2 chemisorption (T_{red} = 250 °C).
[b] Mol of consumed H_2 by mol of Pd, during TPR experiments (T_{ox} = 300 °C).

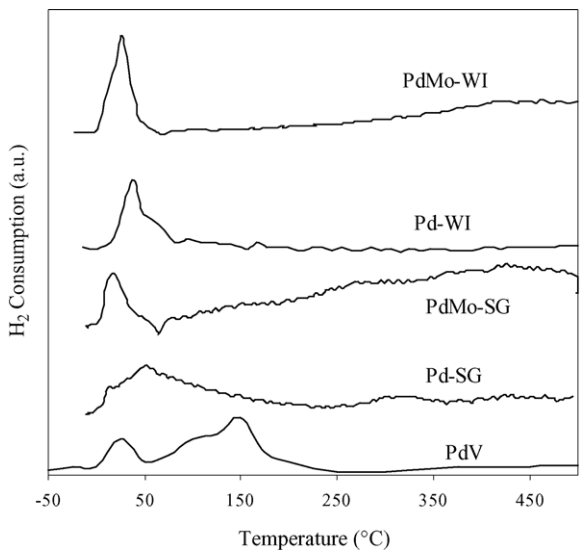

Fig. 1. TPR profile for the studied catalysts. Pre-treatment: oxidation in air at 300 °C.

palladium hydride. This hydrogen evolution peak is slightly insinuated in Pd-WI and PdMo-WI samples, and is bigger for PdMo-SG catalyst. This correlates well with the Pd particle size, since the hydride formation is a volumetric phenomenon [22]. Concerning the Pd-SG sample, it seems that the hydride decomposition signal overlaps the H_2 consumption peak.

PdMo-WI presents a very low hydrogen consumption just before 500 °C, due to partial reduction of MoO_3. The hydrogen consumption peak is small as a result of the low Mo loading. Under these conditions, the interaction between Mo and alumina is strong and the reduction of MoO_3 requires higher temperatures [23–25].

When Pd catalysts are modified with molybdenum, the peak corresponding to PdO reduction shifts to lower temperatures (Fig. 1). This has been previously reported for Pd-Mo catalysts [26,20]. The molybdenum addition causes an easier reduction of PdO. On the other hand, the difference in the temperature in the reduction of PdO in Pd-SG and Pd-WI samples (58 and 38 °C, respectively) is significant. In this case, it could be considered that the difference is a consequence of the different supports and their interaction with Pd. Hydrogen consumption peak of Pd-SG sample is broader than the profile of Pd-WI. Broad reduction peaks are associated with the presence of particles of various sizes.

Regarding Pd-V catalyst, the low temperature peak, at approximately 22 °C, is assigned to the reduction of PdO. The reduction profile presents an additional hydrogen consumption peak at about 150 °C, which is assigned to a partial reduction of VO*x* species due to close contact with the noble metal [9]. The peak is well defined, which is an indication that the palladium–vanadium interaction is higher. Comparing the high temperature peaks of V monometallic samples [9] with that of bimetallic sample, it is clear that the interaction lowers the vanadia reduction temperature by 300 °C approximately.

Table 2 shows that the H_2/Pd consumption ratio (for PdO peak) is greater than the corresponding stoichiometric value for all the samples except PdMo-SG. A similar observation in Pd/γ-Al_2O_3 catalysts [27], with a Pd concentration below 1%, was explained by considering a Pd oxidation state higher than Pd^{2+}, or the existence of a highly dispersed and oxygen-rich species. Regarding Pd-V sample, 50% of palladium is not reduced. Thus, the reduction of VO*x* takes place at the expense of a fraction of Pd that remains in an oxidized state. Another possibility is that the fractions of palladium not reduced at a low temperature, become reduced along with the VO*x* species that is at a higher temperature. Unfortunately we cannot distinguish between these two alternatives.

3.2. Catalytic activity measurements

3.2.1. Mass transfer effects

The volumetric gas–liquid mass-transfer coefficient, K_la, was separately measured at an excess of catalyst load (more than 3%) [13]. The value obtained is in the range 0.3–0.5 s^{-1} and can be considered acceptable [28].

The Weisz–Prater criterion, Eq. (1), was used to evaluate the intraparticle diffusion limitations:

$$\Phi_i = \frac{(-r_{\mathrm{obs},i})\rho_p R_p^2}{D_{\mathrm{eff},i} C_i} \quad (1)$$

where *i*: H_2, TAG.

A value of Φ_i smaller than 0.03–0.7 means that mass-transfer limitation for the unknown kinetics is negligible. The hydrogen concentration in the liquid was calculated from Andersson et al. [29]. Intraparticle diffusion coefficients for the catalysts were taken as $D_{H_2} = 1.2\ 10^{-8}\ m^2\ s^{-1}$ and $D_{TAG} = 1\ 10^{-10}\ m^2\ s^{-1}$ [29]. The density of sunflower oil was determined from [40] as $\rho_{TGA} = 0.866$ g/ml, and tortuosity and porosity were 4 and 0.5, respectively.

In the present experiments, the numerical value of the Weisz–Prater modules of H_2 and TAG always remained above 15 (Table 3).

The composition of the fatty acids at the end of the hydrogenation process is showed in Table 4. In all the cases, there was an increase in the concentration of stearic acid (C18:0) and a decrease in linoleic and linolenic acids (C18:2c and C18:3c) due to the saturation of the double bonds.

As a consequence of the hydrogenation, both reactions of geometric isomerization (*cis–trans*) and positional

Table 3
Values of the Weisz–Prater modulus (Φ) for some catalysts.

Catalysts	r_{obs} (mol s^{-1} kg^{-1} catalyst)	d_p (m)	Φ (H_2)	Φ (TAG)
Pd-WI	0.25	2.11×10^{-4}	233.8	88.1
Pd-SG	0.23	1.41×10^{-4}	48.2	18.2

Table 4
Hydrogenation of sunflower oil:molar fraction (%)

Fatty acids	Sunflower oil	Hydrogenation over			
		Pd-WI	PdMo-WI	Pd-SG	PdMo-SG
C16:0	6.1	5.7	5.4	5.9	5.95
C18:0	3.4	11.1	14.1	12.8	8.25
C18:1t	0.0	35.0	48.3	53.4	37.16
C18:1c	35.2	43.3	28.6	26.5	45.57
C18:2t[a]	1.4	1.0	0.5	0.3	0.31
C18:2c	52.6	3.5	3.0	1.0	2.70
C18:3c	0.4	0.0	0.0	0.0	0.00
C20:0	0.1	0.2	0.1	0.1	0.06
C22:0	0.1	0.0	0.1	0.1	0.00
Trans	1.4	36.0	48.7	53.7	37.5
IV	124.9	75.1	72.1	70.9	75.4

Experimental condition: $T = 100\,^{\circ}C$, $P = 60$ psi
[a] Sum of *cis–trans*, *tran–cis* and *trans–trans*.

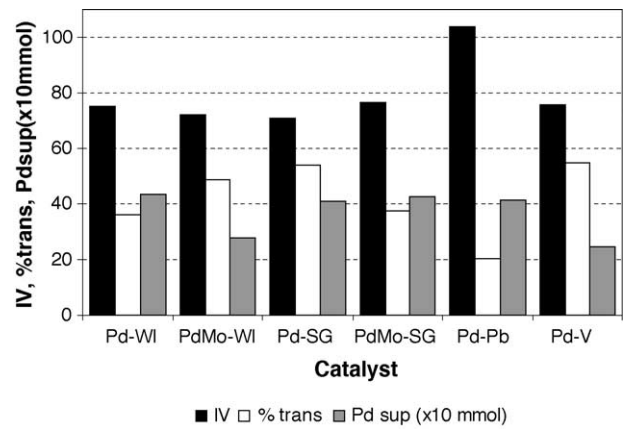

Fig. 2. Hydrogenation of sunflower oil: iodine number (IV), percentage of *trans*-isomer and superficial palladium. Reaction time = 60 min.

isomerization took place. As the present work is focused on the control of the *trans*-isomers, the geometrical isomers are presented in Table 4 without taking into account the position of double bond in the fatty acid chain, only distinguishing between *cis*- and *trans*-isomers (Scheme 1 [30]).

The iodine value (IV) of an oil or fatty acid is the weight of iodine with which it will combine, expressed as a percentage of its own weight [31]. IV expresses the degree of unsaturation of the oil as:

$$\mathrm{IV} = \frac{\text{g of iodine absorbed}}{100\,\text{g of oil}} \tag{2}$$

Thus, during the hydrogenation process, the IV of the sunflower oil decreases, as shown in Table 4. The initial IV is 124.9, and diminishes to 75.1 when the catalyst used is Pd-WI. The lowest IV value is 70.9 when Pd-SG is used. For bimetallic catalysts, the final IV values were 72.1 and 75.4 for PdMo-WI and PdMo-SG, respectively.

Fig. 2 objectively presents the information summarized in Table 4. From these data, it can be carried out a comparison among the various studied catalysts. With respect to the Pd monometallic catalysts it was found that, at similar IV value and Pd surface area, Pd-SG generates more *trans*-isomers than the Pd-WI sample (53.7% and 36%, respectively). Both catalysts were prepared using the same technique of impregnation and metallic precursor ($Pd(C_5H_7O_2)_2$). In addition, Pd-WI and Pd-SG present similar metal particle sizes: 2 and 2.8 nm, respectively (calculated according to [32]). Thus, it can be considered that the cause of the difference in the selectivity to trans is the morphologic properties of the support, presented in Table 1. One difference between samples is the specific surface area, larger for Pd-SG. It was reported that a large surface area favors isomerization reactions, due to the greater accessibility to the active sites [33]. Another important aspect is the pore size distribution. According to Balakos and Hernández [34], pores of small diameter favor the saturation of the fatty acid, since the successive hydrogenation is facilitated by the difficulty in the mobility of the bulky molecule. The pore average size for the supports used in this work is 63.6 and 97.7 Å for Pd-SG and Pd-WI, respectively, whereas the concentration of C18:0 (stearic acid) is 12.8 and 11.1 for Pd-SG and Pd-WI, respectively, in agreement with the previous observation.

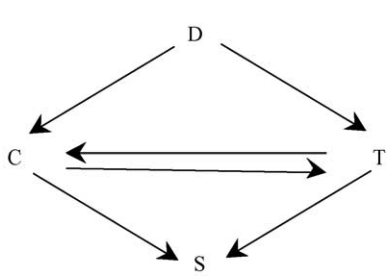

Scheme 1. Diene hydrogenation scheme [30]. D: dieno, C: *cis*-monoene, T: *trans*-monoene, S: saturated.

When comparing in Fig. 2 the hydrogenated oil samples using Pd-WI and PdMo-WI catalysts, it can be observed that both catalysts are similarly active (similar IV), for a smaller amount of exposed Pd. Selectivity to *trans*-isomers also increases in the PdMo-WI catalyst. On the other hand, Pd surface area is smaller in the bimetallic sample.

According to O_2 sorption isotherm previous results [35], after a reduction treatment of an alumina supported Pd-Mo catalyst, molybdenum species are present as Mo^{+5}, which has one unpaired d-electron ([Kr] $4d^1 5s^0$). It has been suggested [36] that unpaired d-electrons are necessary to bind the adsorbing molecule to the surface in a weakly-held precursor state, from which it then passes to the final strongly-bonded state. The convenience of this intermediate state may operate to reduce the activation energy for adsorption to a suitably low value. Thus, this would explain the change in activity for the bimetallic catalyst, which is able to sustain the same activity than its monometallic counterpart even though the exposed Pd surface is half that of Pd-WI.

The availability of this intermediate state may serve to reduce the activation energy for adsorption to a conveniently low value, producing the final state strongly connected

on Pd active sites, following with the formation of the half-hydrogenated intermediate according to the well-known Horiuti–Polanyi mechanism [37].

Concerning the PdMo-SG catalyst, the reaction proceeds to assort the same degree than Pd-SG (at the same reaction time). The selectivity toward *cis*-isomers increases in the bimetallic sample. Moreover, this sample shows a lower production of saturated components (C18:0). This fact is not an expected result in view of its pore size distribution (63.6 and 34.9 Å for Pd-SG and PdMo-SG, respectively). Thus, these results would be the consequence of a Mo effect.

The disparity in the results between PdMo-WI and PdMo-SG indicate that the promotion effect of Mo is a complex phenomenon, which seems to be influenced by the Mo concentration and catalyst preparation. This issue will be focus of future research. Furthermore, and indicating the positive effect of Mo in sol–gel catalysts, comparing Pd-SG and PdMo-SG samples it is noted an improvement in the *cis*-isomers selectivity by Mo addition.

Regarding the Pd-Pb/γ-Al_2O_3 sample, the IV value is higher than Pd-WI (104 versus 75), indicating a lower hydrogenation activity. As a consequence of this, the percentage of *trans*-isomers is lower too.

On the other hand, Pd-V/γ-Al_2O_3, having a smaller amount of exposed Pd than Pd-WI, presents a similar activity but a higher selectivity to *trans*-isomers.

The above observations can be explained as a function of their characterization. In Pd-Pb/γ-Al_2O_3 sample, Pb alloys with Pd [38,39], changing interatomic spacing Pd-Pd. This is important taking in account that there is considerable evidence that the hydrogenation of an ethylenic compound must be preceded by two-point adsorption of the carbon atoms on either end of the double bond [40]. This requirement would impose certain dimensional limitations on the space lattice of any catalytically active metal. Actually, the metals that are at all effective in the hydrogenation of double bonds (Ni, Co, Fe, Cu, Pt, and Pd) have interatomic spacing close to that (27.3 nm) calculated as optimum for such two-point adsorption.

In the case of Pd-V/γ-Al_2O_3 catalyst, vanadium strongly interacts with γ-alumina and is molecularly dispersed on the support as VO*x* species [41]. These VO*x* species are anchoring sites for the $Pd(C_5H_7O_2)_2$ precursor due to the low concentration of OH groups expected on the alumina support after V addition. After calcination step, Pd particles remain on V monolayer. So, this catalyst could be described as Pd particles (with a low dispersion) supported on a VO*x* monolayer. With these facts in mind, changes in the hydrogenation activity between Pd-V and Pd catalysts could be explained in terms of a model, which places a large concentration of negative charge density in the region between the carbon atoms in the double bond and there is Pd particle supported in a deficient electron VO*x* surface. Thus, and in similar way than for Pd-Mo catalyst, VO*x* could facilitate the formation of an adsorbed initial state, after which the hydrogenation would take place on the Pd surface.

4. Conclusions

This study of Pd monometallic catalysts prepared by wet impregnation of γ-Al_2O_3 and alumina sol–gel shows that, for the same IV and Pd surface, Pd-SG generates more *trans*-isomers than Pd-WI sample. This could be attributed to differences in the support morphology.

Regarding bimetallic catalyst, for a smaller amount of exposed Pd, the Pd-Mo/γ-Al_2O_3 and Pd-V/γ-Al_2O_3 catalysts present the same activity compared with the respective Pd monometallic catalyst, and increase the selectivity to *trans*-isomers. The molybdenum and vanadium promoting effect could be a consequence of the formation of an adsorbed initial state, after which the hydrogenation would take place on the Pd surface.

On the other hand, the lower hydrogenation activity showed by Pd-Pb/γ-Al_2O_3 sample would be the consequence of a certain dimensional limitations on the space lattice of Pd for hydrogenation of double bonds due to the formation of a Pd–Pb alloy.

The sol–gel Pd-Mo sample was the most effective catalyst regarding the cis-isomers selectivity and reveals the route for future research.

Acknowledgements

The authors thank the Universidad Nacional del Sur (UNS) and the Consejo Nacional de Investigaciones Científicas y Técnicas (CONICET) for the financial support.

References

[1] J. Coenen, J. Am. Oil Chem. Soc. 3 (1976) 382.
[2] D. Kromhout, A. Menotti, B. Bloemberg, C. Aravanis, H. Blackburn, R. Buzina, A. Dontas, F. Fidanza, S. Giampaoli, A. Jansen, A. Et, Prev. Med. 24 (1995) 308.
[3] D. Jovanovic, R. Radovic, L. Mares, M. Stankovic, B. Markovic, Catal. Today 43 (1998) 21.
[4] G. Carturan, G. Facchin, G. Navazio, La Chimica E L'Industria 65 (1983) 687.
[5] A. Wright, A. Mihele, L. Diosady, Food Res. Int. 36 (2003) 797.
[6] D. Weishaupt, Ph.D. thesis, University of Erlangen-Nürberg, Alemania, 1999.
[7] E. Draguez, D. Hault, J. Am. Oil Chem. Soc. 61 (1984) 195.
[8] E. Santacesaria, P. Parrella, M. Di Sergio, G. Borrelli, Appl. Catal. A 116 (1994) 269.
[9] C. Neyertz, M. Volpe, C. Gigola, Catal. Today 57 (2000) 255.
[10] A. Pisanu, C. Gigola, Appl. Catal. B 11 (1996) L37.
[11] J. Benson, H. Hwang, M. Boudart, J. Catal. 30 (1973) 146.
[12] G. Tonetto, D. Damiani, J. Mol. Catal. A 202 (2003) 289.
[13] O. Stenberg, N.-H. Schöön, Chem. Eng. Sci. 40 (1985) 2311.
[14] P. Weisz, D. Prater, Adv. Catal. 6 (1954) 143.
[15] A. Pierre, E. Elaloui, G. Pajonk, Langmuir 14 (1998) 66–73.
[16] K. Ishiguro, T. Ishikawa, N. Kakuta, A. Ueno, Y. Mitarai, T. Kamo, J. Catal. 123 (1990) 523.
[17] J. Armor, E. Carlson, P. Zambri, Appl. Catal. 19 (1985) 339.
[18] E. Lesage-Rosenberg, G. Vlaic, H. Dexpert, P. Legarde, E. Freund, Appl. Catal. 22 (1986) 211.
[19] P. Aben, J. Catal. 10 (1968) 224.

[20] L. Konopny, A. Juan, D. Damiani, Appl. Catal. B 15 (1998) 115.
[21] F. Noronha, M. Baldanza, M. Schmal, J. Catal. 188 (1999) 270.
[22] H. Rodriguez Cárdenas, Tesis Doctoral, UNS, 1986.
[23] S. Rajagopal, H. Marini, J. Mazari, R. Miranda, J. Catal. 147 (1994) 417.
[24] L. Wang, W. Hall, J. Catal. 66 (1980) 251.
[25] H. Knözinger, H. Jezioroswski, J. Phys. Chem. 83 (1979) 1166.
[26] M. Schmal, M. Baldanza, A. Vannice, J. Catal. 185 (1999) 138.
[27] T. Hoost, K. Otto, Appl. Catal. A 92 (1992) 39.
[28] E. Santacesaria, P. Parrella, M. Snm Di Serio, G. Borrelli, Appl. Catal. A 116 (1994) 269.
[29] K. Andersson, M. Hell, L. Löwendahl, N.-H. Schöön, J. Am. Oil Chem. Soc. 51 (1974) 171.
[30] K. Hashimoto, K. Muroyama, S. Nagata, J. Am. Oil Chem. Soc. 48 (1971) 291.
[31] F.D. Gunstone, M. Kates, J.L. Harwood, in: F.D. Gunstone, J.L. Harwood, F.B. Padley (Eds.), The Lipid Handbook, second ed., Chapman and Hall, London, 1994.
[32] P. Aben, J. Catal. 10 (1968) 224.
[33] M. Macher, Ph.D. thesis, Chalmer University of Technology, Göteborg, Suecia, 2001.
[34] M. Balakos, E. Hernández, Catal. Today 35 (1997) 415.
[35] A. Eberhardt, E. Benvenutti, C. Moro, G. Tonetto, D. Damiani, J. Mol. Catal. A 201 (2003) 247.
[36] G. Bond, in: G.C. Bond (Ed.), Heterogeneous Catalysis. Principles and Applications, second ed., Claredon Press, Oxford, 1987.
[37] J. Horiuti, M. Polanyi, Trans. Faraday Soc. 30 (1934) 1164.
[38] G. Liu, K.A. Davis, D.C. Meier, P.S. Bagus, D.W. Goodman, G.W. Zajac, Phys. Rev. B 68 (2003) 035406.
[39] M. Volpe, P. Rodriguez, C. Gigola, Catal. Lett. 61 (1999) 27.
[40] R. Allen, M. Formo, R. Krishnamurthy, G. McDermott, F. Norris, N. Sonntag, in: D. Swern (Ed.), Bailey's Industrial Oil and Fat Products, vol. 2, fourth ed., John Wiley and Sons, 1982.
[41] C. Neyertz, C. Gigola, M. Volpe, Appl. Catal. A 277 (2004) 137.